Metrol. Meas. Syst., Vol. 32 (2025), No. 3
DOI: 10.24425/mms.2025.154680

METROLOGY AND MEASUREMENT SYSTEMS
Index 330930, ISSN 0860-8229
www.metrology.wat.edu.pl

COMPARISON OF LOCAL MODE SHIFT AND CUT-OFF WAVELENGTH SHIFT FOR DEMODULATION OF TILTED FIBRE BRAGG GRATING SENSORS

Sławomir Cięszczyk[1)], Krzysztof Skorupski[1)], Patryk Panas[1)], Martyna Wawrzyk[2)]

1) *Department of Electronics and Information Technology, Lublin University of Technology, Nadbystrzycka 38A, 20-618 Lublin, Poland* (✉ *s.cieszczyk@pollub.pl*)
2) *Doctoral School, Lublin University of Technology, Nadbystrzycka 38D/406, 20-618 Lublin, Poland*

Abstract

Tilted fibre Bragg gratings (TFBGs) have a characteristic transmission spectrum in the form of a fine comb of cladding mode resonances. This spectrum changes significantly when the sensor is immersed in a substance with a specific refractive index (RI) value. Surrounding RI (SRI) values can be derived from global shape of the entire cladding mode spectrum or local shape of a single mode. In this article, we present comparisons of two types of TFBG spectra demodulation methods for SRI determination. The first approach to determining the SRI is based on the local wavelength shift of a single mode and a group of cladding modes. As a modification, a differential method of analysis of two modes and two groups of modes (spectral bands) was proposed. As a result, differential methods with better resolution and linearity were obtained compared to single mode analysis. To determine the local shift the centroid, fast phase correlation and cross-correlation methods were used. The global spectrum analysis method with cut-off wavelength determination was used as the second type of demodulation method. The cut-off wavelength shift was determined using the maximum derivative method of the smoothed absolute value of the derivative of the optical spectrum. The best resolution of SRI determination for the local method was $2.4 \cdot 10^{-5}$ RIU, while for the global method it was $1.75 \cdot 10^{-5}$ RIU for the SRI measurement range of 1.333 to 1.361 RIU.

Keywords: tilted fibre Bragg grating, fibre optics sensor, refractive index.

1. Introduction

Tilted fibre Bragg gratings (TFBGs) are sensors developed for use in the measurement of various quantities [1, 2]. However, the most promising application of these structures is the measurement of the refractive index. Refractive index measurements are used to determine the content of various substances such as cholesterol solution concentration [3], paracetamol concentration [4], simultaneous temperature and salinity [5]. The greatest advantage of TFBG gratings is the lack of any physical change in the fibre cladding. This is due to the process of their inscription in optical fibres. Therefore, TFBG sensors have many applications as biosensors for diagnostics and health research [6]. The tilt of the grating planes in the fibre core causes the formation of several dozen cladding modes. Immersing such a structure in a substance having a specific *refractive index* (RI) value changes the spectrum of the cladding mode comb. Increasing the *surrounding refractive index* (SRI) shifts the so-called cut-off wavelength. Successive modes from the side of shorter wavelengths broaden and decrease their amplitude. This is an effect similar to signal smoothing that progresses towards longer wavelengths as the SRI increases. At the same time, all cladding modes undergo a slight shift towards longer wavelengths. This shift is non-linear and smaller for longer wavelength modes. The maximum sensitivity of a single mode, which is a mode at the cut-off wavelength limit, can be 28 nm/RIU, but only in the range of 0.002 RIU [7].

Article history: received April 9, 2025; revised May 14, 2025; accepted July 25, 2025; available online August 6, 2025.

Determination of the (RI) value on the basis of the measured transmission spectrum requires an appropriate demodulation algorithm. Algorithms can be divided into global ones, which use the entire spectrum of cladding modes, and local ones, which use a single resonance spectrum. Amplitude or wavelength shift parameters can be determined. The first algorithm was used to determine the surface area between the upper and lower envelopes of all cladding modes [8]. Global amplitude methods also include the calculation of the spectral length parameter [9]. Global spectral variations can also be localised to a specific wavelength. Algorithms using this property look for shifting the cut-off wavelength with increasing SRI [10, 11]. Local techniques include the analysis of a single mode spectral shift [12]. An interesting method of using the shifts of many resonant peaks is to use a greater shift of the peaks for shorter wavelengths in relation to the peaks for longer wavelengths [13]. Among the methods using spectrum transformations the Fourier transform was used to determine the SRI as a method of pre-processing data [10]. The shape of the Fourier amplitude spectrum can also be used to determine the SRI [14]. In addition to the methods presented, there are a few others that are discussed in our previous works and in the references.

The shift of the position of the spectrum shapes is determined by two basic methods: centroid and phase analysis in the frequency domain. The fast phase correlation method [15] is used to demodulate the *fibre Bragg grating* (FBG) with high accuracy. Both methods derive information from subpixel resolution. The FBG spectrum has one peak, which changes its position under the influence of the interacting quantity, but maintains its shape. Demodulation of the FBG spectrum consists in searching for the shift of the spectrum peak. The phase correlation method works well in the case of a shift of a single peak measured in the reflection mode. The TFB grating has several dozen modes and is measured in the transmission mode. The TFBG spectrum therefore requires appropriate transformation before applying the demodulation methods used for classical FBGs. In the case of local demodulation methods, additional spectrum preprocessing consists in averaging the shapes and shifts of several modes. The spectrum processed in this way can be directly analysed using methods known from the demodulation of FBG grating spectra. In the second case, the shift of the mode group is analysed, which can be determined using the analysis of the main cross-correlation peak. The correlation is calculated between the spectrum for the known reference SRI value and the spectrum for the sought SRI value.

Single mode shift analysis methods are temperature sensitive. Counteracting this phenomenon is the use of offset correction using information from the Bragg peak. However, for some reason this peak cannot be clearly visible due to an incorrect TFBG tilt angle or spectra measurement issues. For gratings with a tilt angle of 6-8%, the Bragg mode has a very small amplitude compared to the amplitudes of cladding modes. Demodulation of such a mode is therefore ineffective. Then the low order cladding mode peaks farther from the cut-off wavelength can be used instead of the Bragg peak as their SRI sensitivity is minimal. They can therefore be used to correct the shift of modes lying closer to the cut-off wavelength. Several such modes can also be used for correction at the same time [16]. The use of the grating spectrum by dividing it and determining the shift difference is an algorithmic differential method. Its main advantage is the lack of a second separate measuring channel dedicated to temperature correction.

The purpose of this article is to discover the properties of the presented methods and evaluate them for determining the SRI based on the TFBG spectrum. The range of the SRI values measured was selected to compare local and global methods. Proper comparison is only possible for simultaneous analysis of the same spectral measurements. The main novelty achieved in the article is the comparison of the resolution of local and global methods for the same measurement system and the range of measured SRI values. For local methods, new methods of spectrum processing were used, consisting in averaging the shift of several modes.

Additionally, a differential method was used for two groups of modes. For both local and global methods, the feature enhancement method was used to raise the processed spectrum to the second power (power transformation).

2. **Shift demodulation methods of a single mode and a group of modes**

Demodulation algorithms using phase changes calculate the shift difference between the two measured spectra. The appropriate part of the spectrum measured in distilled water was selected as the reference vector R_1 for calculations. If the grating is immersed in a solution with a higher SRI coefficient, the measurement vector R_2 can be defined as:

$$R_2(\lambda) = R_1(\lambda - \Delta\lambda), \tag{1}$$

where λ is the wavelength and $\Delta\lambda$ is the shift between R_1 and R_2. The simplest algorithm for determining the wavelength shift is the centroid algorithm, which is equivalent to calculating the centre of gravity of the FBG grating spectrum shape:

$$\lambda_B = \frac{\sum_n \lambda_n \cdot R(\lambda_n)}{\sum_n R(\lambda_n)}. \tag{2}$$

We can now compute the Fourier transform of both vectors:

$$X_1(k) = \sum_{n=0}^{N-1} R_1(n) \cdot e^{\frac{-2\pi jnk}{N}}, k = 1,2, \dots (N-1), \tag{3}$$

$$X_2(k) = \sum_{n=0}^{N-1} R_2(n) \cdot e^{\frac{-2\pi jnk}{N}}, k = 1,2, \dots (N-1), \tag{4}$$

where N is the length of both the R_1 and R_2 vectors and k is the index of Fourier spectra vectors. The Fourier transform can be represented as an amplitude modulus and a phase ϕ:

$$X_2(k) = |X_2(k)| \cdot e^{-j\phi_2(k)}. \tag{5}$$

We analyse the range of the optical spectra that does not change significantly and the modes that are only shifted. The change in the shape of a specific mode can be quantitatively assessed by analysing the change in the mode amplitude and its half-width. This means that the moduli of the Fourier spectrum amplitudes will be the same:

$$|X_2(k)| = |X_1(k)|. \tag{6}$$

Only the phases of both Fourier spectra will change:

$$\Delta\phi(k) = \phi_2(k) - \phi_1(k) = \frac{2 \cdot \pi \cdot k \cdot \Delta\lambda(k)}{N \cdot \delta}. \tag{7}$$

where δ is the wavelength resolution. The actual measurement vectors differ not only in their position, but also in their shape. This means that only a certain number M of the initial frequency components has phase values reflecting the shift of the considered shapes [15]:

$$\Delta\lambda(k) = \Delta\phi(k) \cdot \frac{N \cdot \delta}{k \cdot 2 \cdot \pi}, k = 1,2, \dots M < N. \tag{8}$$

The estimation of the spectral shape shift value can be determined using the median of the shifts resulting from M initial components [13]:

$$\Delta\hat{\lambda} = \text{median}(\Delta\lambda(k)), k = 1,2, \dots M. \tag{9}$$

The spectral shift can also be calculated as the maximum correlation between two spectra:

$$XC_j = \sum_{i=0}^{N-1} R_0(\lambda_i) R_1(\lambda_{i+j}), j = 1,2, \dots (2N-1). \tag{10}$$

The wavelength shift based on the calculated cross-correlation function can be calculated using the

centroid algorithm or the fast phase correlation algorithm.

The last algorithm used to enhance the spectral features and cross-correlation function is the algorithm based on raising the spectra to a power of P [17]:

$$G(\lambda) = R^P(\lambda). \tag{11}$$

This relatively simple mathematical operation is called power transformation and increases the signal-to-noise ratio [18]. Additionally, power transformation narrows the spectrum peak and reduces any asymmetry in its profile. Power transformation is also used to improve the properties of time windows [19, 20]. All algorithms and signal processing methods were developed by the authors using the *Matlab* programing environment.

3. **Wavelength shift of the individual cladding modes**

For the measurements, we used a grating inscribed in a standard optical fibre using the phase mask method. Before the inscription process, the optical fibre was subjected to a hydrogenation process in order to increase its sensitivity to ultraviolet light from the excimer laser. The grating has a tilt angle of 6 degrees obtained by rotating the phase mask during the writing process. The transmission spectrum of the grating immersed in water-glucose solutions was measured. The refractive index values were measured using a reference laboratory refractometer. The refractive index was measured in the range of 1.333 to 1.361 for nineteen values and twenty repetition. The measurements were performed using an *Optical Spectrum Analyser* (OSA) Yokogawa AQ6370D and a *Superluminescent Diode* (SLD) as the radiation source. The measurements were performed in transmission mode with a spectral resolution of 0.004 nm. The diagram of the measurement system is shown in Fig. 1.

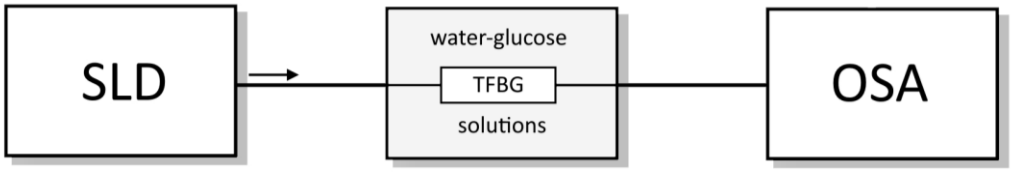

Fig. 1. Drawing of the measuring system of the TFBG grid immersed in a liquid with a specified SRI value.

Changes in the TFBG grating spectrum under the influence of changes in the surrounding refractive index can be divided into global and local. Global changes in the shape of the TFBG spectrum are shown in Fig. 2. Such changes are related to the leakage of successive cladding modes as a result of shifting the cut-off wavelength. The largest changes in amplitude and position occur for modes lying c*lose to the cut-off wa*velength. Local changes are shifts of individual cladding modes with wavelengths longer than the cut-off wavelength (Fig. 3).

The shift of individual modes is greater for modes with shorter wavelengths. The third figure shows two modes, one of which lies near the cut-off wavelength and the other 19 nm further away. The shift of the peak at wavelength 1511.2 nm is greater than the shift of the peak at 1530.4 nm. Shorter wavelength modes are higher order modes. Such modes penetrate deeper into the liquid surrounding the optical fibre cladding, hence their greater sensitivity to SRI changes. A comparison of the shift values of several cladding modes is shown in Fig. 4. Nonlinearity for the most sensitive curves can be up to 30%.

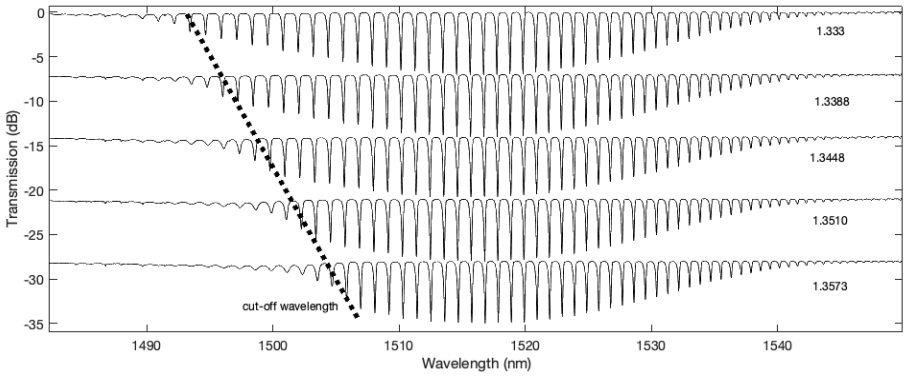

Fig. 2. Global changes of the TFBG spectrum under the influence of changes in the SRI value.

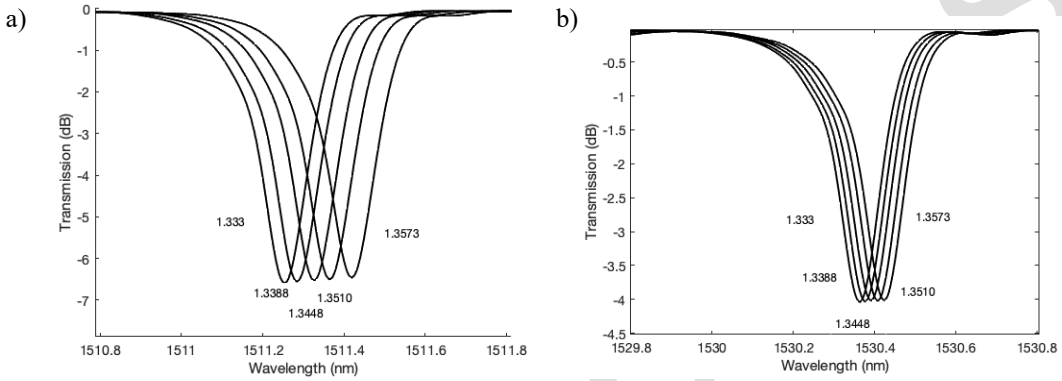

Fig. 3. Spectra of two cladding modes shifted under the influence of a change in the SRI coefficient, a) mode at 1511.2 nm, b) mode at 1530.4 nm.

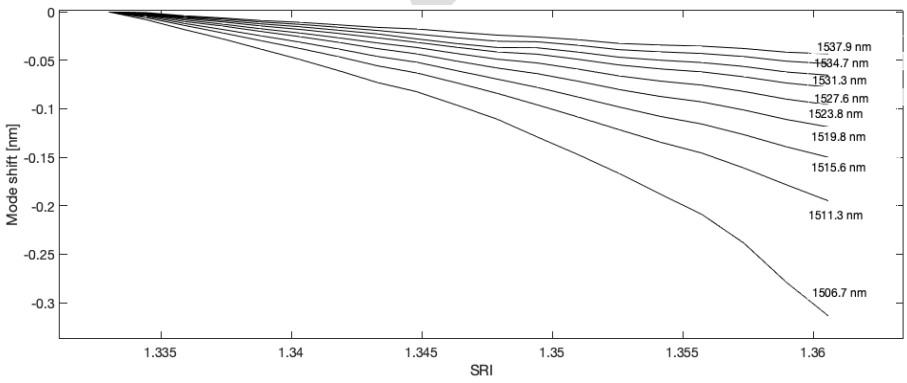

Fig. 4. Wavelength shift values for several modes in the 1474-1505.3 nm range.

Single modes that are located at a certain distance from the cut-off wavelength do not undergo significant changes in shape (Figs. 5 and 6 wavelengths beyond 1505 nm). The spectra of these resonance peaks meet the conditions for use in the analysed method. In order to analyse a single peak, a fragment of the spectrum must be properly chosen. In Fourier analysis, special shapes called windows are used for this. They have the property of reducing spectrum leakage in the frequency domain. During the analysis of the algorithms, several types of windows were tested and finally the Hanning window was selected. As the centre of the $W(m)$ window, the peak wavelength of a given mode for the middle value of the SRI range was selected (Fig. 5).

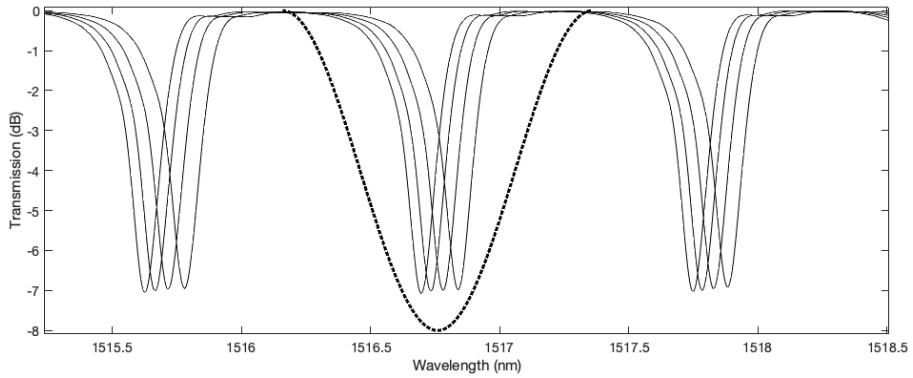

Fig. 5. The method of cutting a part of the spectrum using the apodising window.

a)

b)

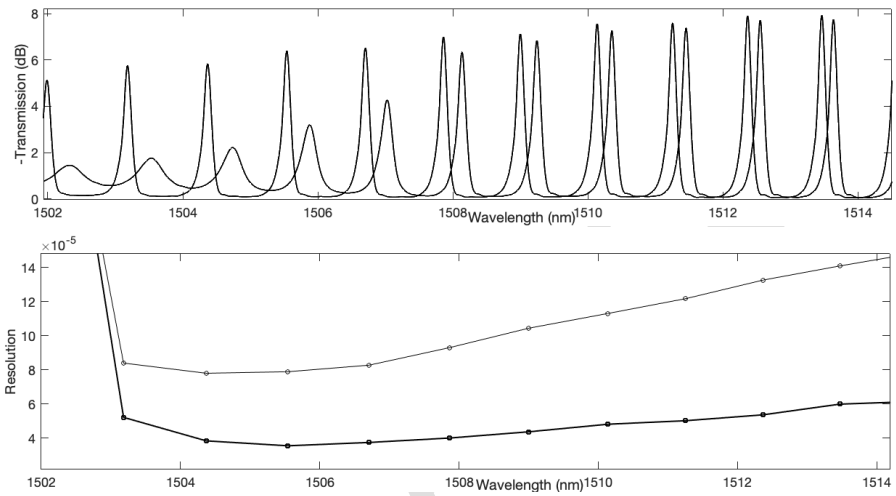

Fig. 6. a) Part of the spectrum for the two SRI values measured, b) SRI measurement resolution for several cladding modes.

The fast phase correlation method was used for subsequent cladding modes. Fig. 6a shows the mode spectra for the two extreme SRI values measured. We calculate the resolution parameter by repeated measurements [21]. Resolution is calculated as the standard deviation of the refractive index value determined from twenty repeated measurements of the spectrum. The best measurement resolution is shown by modes near the cut-off limit in the range of 1503-1508 nm. For subsequent modes above the wavelength of 1509 nm, the resolution value slightly deteriorates. Subsequent resolution calculations were performed for individual modes with wavelength shift correction. The mode with the wavelength of 1535.5 nm was used for correction. The calculated resolution value decreased about twice (Fig. 6b).

The transmission spectrum of the grating has several tens of cladding modes. In order to simultaneously use information from several modes, the input signal for the algorithm should be properly prepared. For this, the sum of the shifted modes can be used:

$$T_a(m) = \frac{1}{N}\sum_{n=0}^{N-1} T(m + k_n) \cdot W(m), \tag{12}$$

where m is the index of the spectrum vector T, W is the cutting window and k_n is the shift of subsequent modes.

At the same time, the shift of each mode k_n is slightly different and determined for the spectrum measured for the middle value of the considered SRI range (Fig. 7). Individual values of k_n differ from each other due to uneven distances between modes. This resulted in an averaged mode, with an averaged amplitude change and an averaged wavelength shift. At the same time, in order to take advantage of the advantages of the differential method, the modes

presented in Fig. 7 were summed up. As the basic modes, those in the range of 1504-1521 nm were selected. Modes in the spectral range of 1526-1539 nm were used for correction in the differential method (Fig. 8). The basic set contains 16 modes, the correction set 18. A valuable property of such a method is the more linear dependence of the differential shift on the SRI (Fig. 8). The resolution of the method for such prepared data (peak averaging) is $3.4 \cdot 10^{-5}$ RIU.

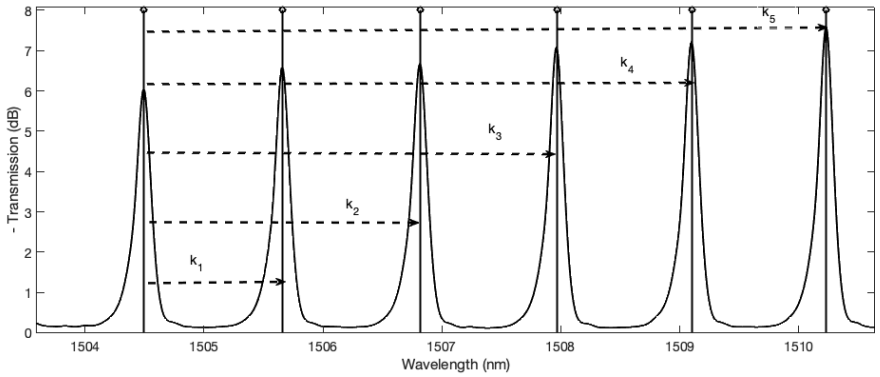

Fig. 7. A method of creating an average peak as a sum of shifted resonance peaks.

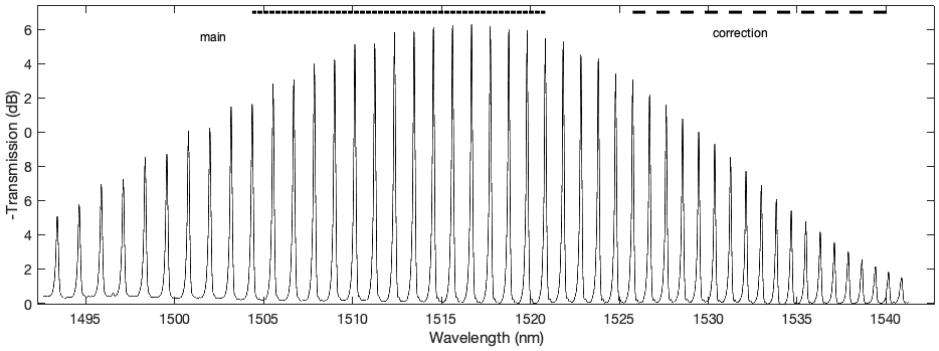

Fig. 8. The spectrum of selected cladding modes.

The averaged modes for the two extreme values are shown in Fig. 9. Figure 9a shows the mode averaged based on the modes from the fundamental spectrum, while Fig. 9b shows the mode averaged from the modes of the correction spectrum. The amplitude of the fundamental mode decreases, because it consists of modes at the cutoff boundary and after the cutoff. Such modes decrease their amplitude and are subject to broadening.

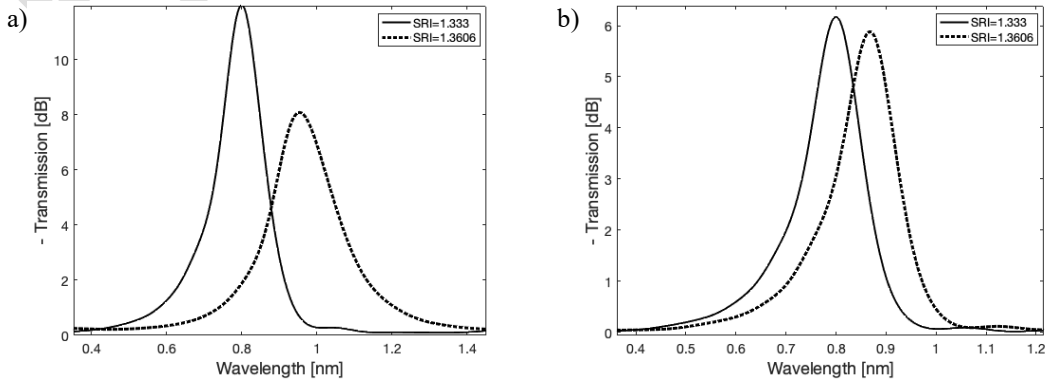

Fig. 9. Averaged modes for two parts of the spectrum, a) the basic part of the spectrum, b) the part of the spectrum to be corrected.

Figure 10 presents the characteristics of the dependence of the wavelength shift difference on the SRI. The first two differences are calculated directly for the averaged modes shown in Fig. 9 using the centroid and *fast phase correlation* (FPC) algorithms. The next two characteristics show shifts calculated after previously performing cross-correlation. These characteristics for both algorithms (centroid and FPC) overlap.

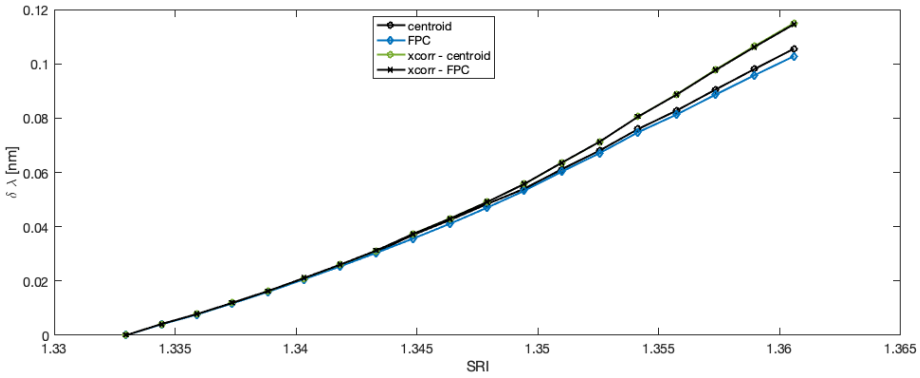

Fig. 10. Dependence of the shift of the averaged mode on the SRI value.

Figure 11 shows the value of spectral resolution depending on the power to which the spectrum is raised for direct methods and the cross-correlation function for correlation methods. A significant decrease in the resolution value is noticeable, especially for calculations performed with the centroid method, both directly and after cross-correlation. The minimum resolution value was $2.4 \cdot 10^{-4}$ RIU for the algorithm consisting of cross-correlation and centroid. Computing the correlation improves the resolution for both algorithms of calculating the shift.

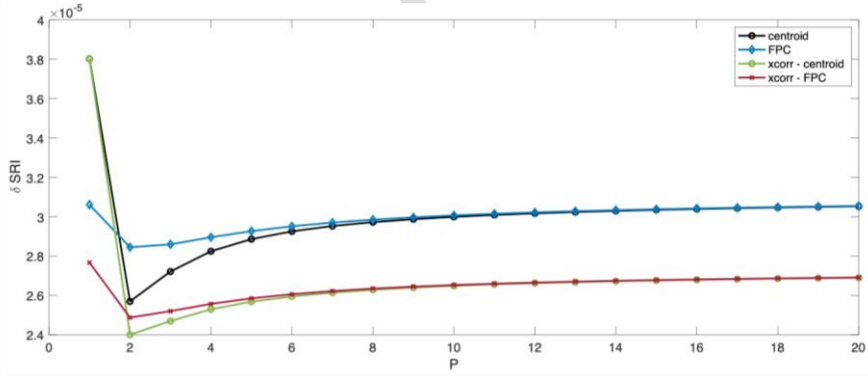

Fig. 11. Resolution of SRI determination as a function of the power value *P* for the 4 analysed demodulation methods.

The average shift of the mode group can also be obtained by calculating the cross-correlation of a specific spectrum range. The correlation is calculated with the reference spectrum, which is measured for the SRI of distilled water. Figure 12 shows the autocorrelation function of the spectrum measured for SRI = 1.333. Part 11a shows the autocorrelation of the basic part of the spectrum, while part 11b shows the spectrum used for offset correction. The autocorrelation has a typical shape characteristic of a periodic or almost periodic signal. Figure 13 shows the main peak of cross-correlation between the spectrum measured for distilled water with two spectra. The first is another spectrum also measured for distilled water and the second is measured for the SRI with a value of 1.3606. The dependence of the shift difference between the cross-correlation function for the basic and correction spectrum ranges is shown in Fig. 14.

The characteristics for both algorithms (centroid and FPC) overlap. Resolution from the value of the power factor P is at a similar level as calculated for calculating correlations for averaged modes. Raising it to the second power significantly reduces the resolution calculated for the centroid algorithm from $4.3 \cdot 10^{-5}$ RIU to $2.5 \cdot 10^{-5}$ RIU, but only slightly for the FPC algorithm from $2.6 \cdot 10^{-5}$ RIU to $2.5 \cdot 10^{-5}$ RIU. The best resolution result obtained is $2.5 \cdot 10^{-5}$ RIU and this is a result at a similar level as for the mode averaging method. Values of the power of P larger than two are not beneficial because they result in increased resolution values for both algorithms.

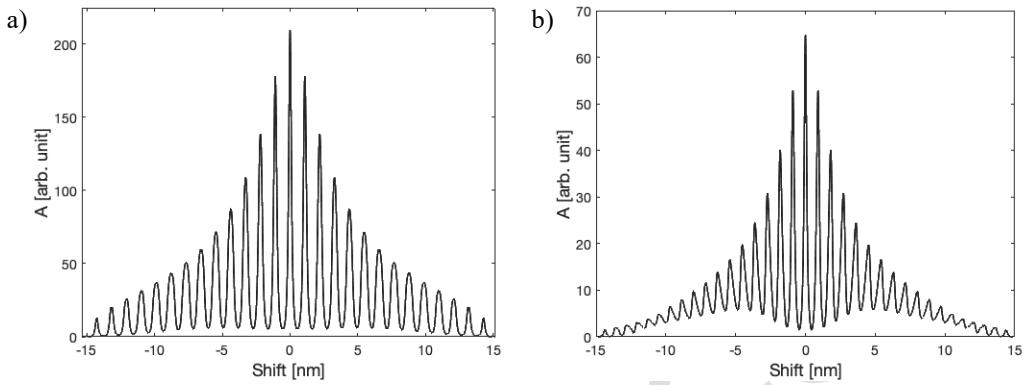

Fig. 12. Comparison of the autocorrelation function for two parts of the spectrum – basic and correction.

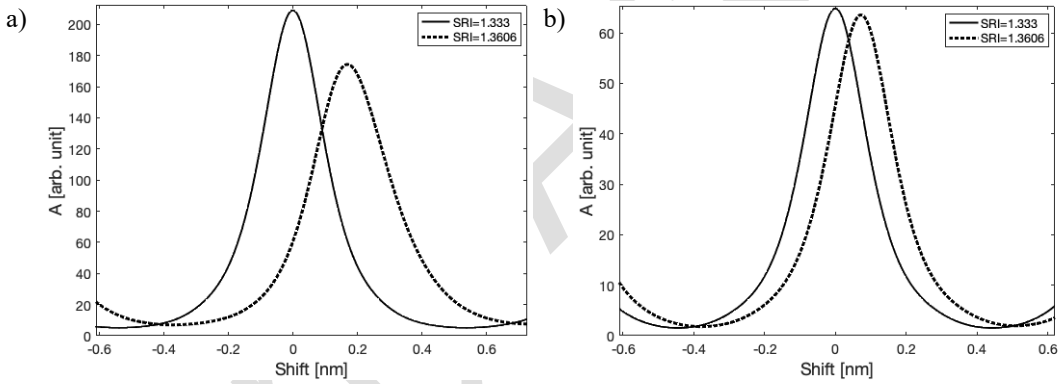

Fig. 13. Comparison of the central part of the autocorrelation function for two parts of the spectrum – basic and correction.

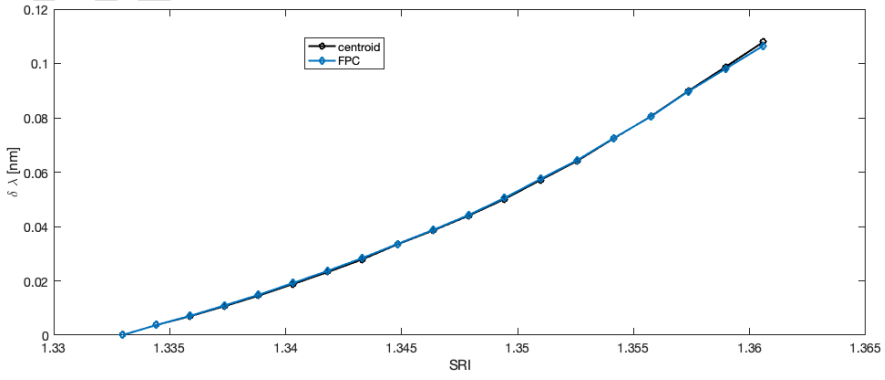

Fig. 14. Dependence of the main lobe shift of the cross-correlation part of the spectrum on the SRI value.

4. **Cut-off wavelength shift determination**

Precise determination of the cut-off wavelength based on the TFBG spectrum is possible only for selected SRI values, for which the cut-off boundary is exceeded by a specific mode. This is due to the fact that such a mode stops shifting and its amplitude begins to decrease. The position of the cut-off wavelength between modes can only be approximated. For measurements of SRI values based on the cut-off wavelength, calibration must be performed. In such a case, it is not necessary to precisely determine the cut-off wavelength, but to shift it relative to the reference spectrum. Determination of the cut-off wavelength shift can be performed in several ways. In each case, the use of several digital signal processing algorithms is required. In this article, we used the initial differentiation of the spectrum. Thus, we eliminate the constant component and the slowly changing components of the spectrum, which do not carry information. Then we calculate the absolute value of the differentiated spectrum. In the next step, we use a non-causal filter with a finite impulse response. Such a filter does not shift individual components of the spectrum. In our calculations, we used a filter with a Gaussian impulse response shape. In the next step, we calculate the derivative (first difference) (Fig. 15b) of the previously smoothed spectrum (Fig. 15a). The position of the cut-off wavelength was determined using the centroid algorithm. The dependence of the cut-off wavelength shift on the SRI is shown in Fig. 16. The characteristic is linear and has a determination coefficient R^2 of 0.9994. Raising the processed spectrum to the second power reduces the resolution value from 1.97·10-5 to 1.75·10-5 RIU. This is a noticeable change, but it is not significant. As for the previous algorithms, increasing the power of P above 2 does not improve the resolution value.

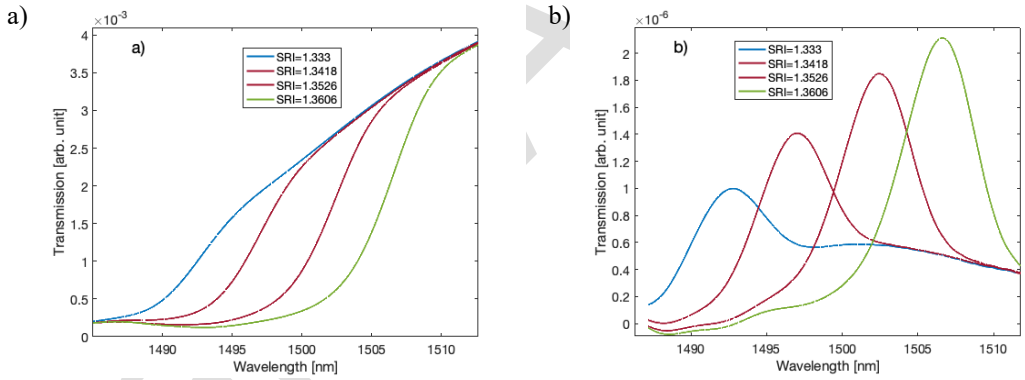

Fig. 15. Smoothed absolute value of the derivative of the optical spectrum a) and its derivative b).

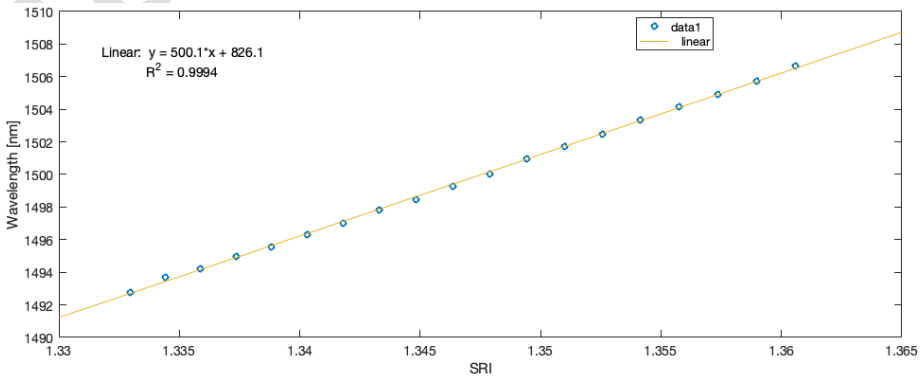

Fig. 16. Dependence of the cut-off wavelength on the SRI value.

5. **Conclusions**

We performed a comparison of the properties of the local and global wavelength shift algorithms. The local shift was determined by two methods: centroid, fast phase correlation and its combination with cross correlation. Three differential data configurations were used. These are differences in shifts of individual peaks, differences in shifts of averaged peaks in certain spectral ranges, and differences in shifts of two spectral ranges. The big advantage of the differential method of two spectral ranges (mode averaging and direct) is obtaining better linearity of the shift's dependence on the SRI. The resolution of the local method was $2.4 \cdot 10^{-5}$ RIU. However, the global wavelength shift method turned out to be much more advantageous. This method uses the following steps: a differentiating filter, calculating the absolute value, smoothing the signal, and the derivative of the smoothed signal. The global method determining the cut-off wavelength shift is a linear method and its resolution was $1.75 \cdot 10^{-5}$ RIU. In the case of both types of algorithms, it is advantageous to raise the processed spectrum to the second power, which significantly improves the resolution. The sensitivity of the wavelength method is 500.1 nm/RIU and is much higher than the average differential sensitivity of the local method of 3.6 nm/RIU. The comparison of methods is much more favourable for the global method. It is characterised by much higher sensitivity and better resolution of SRI determination. Additionally, the method of determining the cut-off wavelength is linear and allows determining the refractive index in a wider range of values.

Acknowledgements

This work was supported by the Lublin University of Technology (grant number: FD-20/EE-2/301).

References

[1] Kisała, P. (2023). Physical foundations determining spectral characteristics measured in Bragg gratings subjected to bending. *Metrology and Measurement Systems*. https://doi.org/10.24425/mms.2022.142275

[2] Kozieł, G., Harasim, D., Dziuba-Kozieł, M., & Kisała, P. (2024). Fourier transform usage to analyse data of polarisation plane rotation measurement with a TFBG sensor. *Metrology and Measurement Systems*, 369–381. https://doi.org/10.24425/mms.2024.149698

[3] Luo, Y., & Luo, J. (2021). Experimental research on cholesterol solution concentration sensing based on tilted fiber Bragg grating. *Optoelectronics Letters*, *17*(11), 661–664. https://doi.org/10.1007/s11801-021-1030-5

[4] Soares, L., Cruz, P., Novais, S., Ferreira, A., Frezao, O., & Silva, S. (2021). Application of a fiber optic refractometric sensor to measure the concentration of paracetamol in crystallization experiments. *IEEE Instrumentation & Measurement Magazine*, *24*(5), 36–40. https://doi.org/10.1109/mim.2021.9491002

[5] Liu, Z., Liu, Z., Mei, Y., Hu, P., & Li, Z. (2023). Simultaneous demodulation of salinity and temperature assisted by deep learning approach utilizing tilted fiber Bragg Grating and Fabry–Perot-Based sensor. *IEEE Sensors Journal*, *23*(21), 26820–26827. https://doi.org/10.1109/jsen.2023.3316721

[6] Jean-Ruel, H., & Albert, J. (2024). Recent advances and current trends in optical fiber biosensors based on tilted fiber Bragg gratings. *TrAC Trends in Analytical Chemistry*, *174*, 117663. https://doi.org/10.1016/j.trac.2024.117663

[7] Huang, Z., Yang, N., Xie, J., Han, X., Yan, X., You, D., Li, K., Vai, M. I., Tam, K. W., Guo, T., & Xiao, G. (2022). Improving accuracy and sensitivity of a tilted fiber Bragg grating refractometer using cladding Mode envelope derivative. *Journal of Lightwave Technology*, *41*(13), 4123–4129. https://doi.org/10.1109/jlt.2022.3178268

[8] Laffont, G., & Ferdinand, P. (2001). Tilted short-period fibre-Bragg-grating-induced coupling to cladding modes for accurate refractometry. *Measurement Science and Technology*, *12*(7), 765–770. https://doi.org/10.1088/0957-0233/12/7/302

[9] Cięszczyk, S., Harasim, D., & Kisała, P. (2017). A novel simple TFBG spectrum demodulation method for RI quantification. *IEEE Photonics Technology Letters*, *29*(24), 2264–2267. https://doi.org/10.1109/lpt.2017.2768601

[10] Cięszczyk, S., Skorupski, K., & Panas, P. (2022). Single- and Double-Comb Tilted Fibre Bragg Grating Refractive Index Demodulation Methods with Fourier Transform Pre-Processing. *Sensors*, *22*(6), 2344. https://doi.org/10.3390/s22062344

[11] Pham, X., Si, J., Chen, T., Wang, R., Yan, L., Cao, H., & Hou, X. (2018). Demodulation method for tilted fiber Bragg grating refractometer with high sensitivity. *Journal of Applied Physics*, *123*(17). https://doi.org/10.1063/1.5025645

[12] Chan, C., Chen, C., Jafari, A., Laronche, A., Thomson, D. J., & Albert, J. (2007). Optical fiber refractometer using narrowband cladding-mode resonance shifts. *Applied Optics*, *46*(7), 1142. https://doi.org/10.1364/ao.46.001142

[13] Kelly-Richard, A., & Albert, J. (2022). Multiresonant analysis improves the limit of detection of tilted fiber Bragg grating refractometers. *Optics Letters*, *47*(15), 3740. https://doi.org/10.1364/ol.462687

[14] Udos, W., Lim, K., Tan, C., Ismail, M. N., Ooi, C., Zakaria, R., & Ahmad, H. (2020). Spatial frequency spectrum of SPR-TFBG: A simple spectral analysis for in-situ refractometry. *Optik*, *219*, 164970. https://doi.org/10.1016/j.ijleo.2020.164970

[15] Lamberti, A., Vanlanduit, S., De Pauw, B., & Berghmans, F. (2014). A novel fast phase correlation algorithm for peak wavelength detection of fiber Bragg grating sensors. *Optics Express*, *22*(6), 7099. https://doi.org/10.1364/oe.22.007099

[16] Cięszczyk, S., Skorupski, K., & Panas, P. (2024). Analysis of demodulation methods of tilted fibre Bragg gratings based on the local shift of the cladding mode group. *Applied Sciences*, *14*(6), 2458. https://doi.org/10.3390/app14062458

[17] Shalliker, R., Stevenson, P., Shock, D., Mnatsakanyan, M., Dasgupta, P., & Guiochon, G. (2010). Application of power functions to chromatographic data for the enhancement of signal to noise ratios and separation resolution. *Journal of Chromatography A*, *1217*(36), 5693–5699. https://doi.org/10.1016/j.chroma.2010.07.007

[18] Dasgupta, P. K., Chen, Y., Serrano, C. A., Guiochon, G., Liu, H., Fairchild, J. N., & Shalliker, R. A. (2010). Black box linearization for greater linear dynamic range: The effect of power transforms on the representation of data. *Analytical Chemistry*, *82*(24), 10143–10150. https://doi.org/10.1021/ac102242t

[19] Borkowski, J., & Matusiak, A. (2024). Power-of-sine windows as generalized maximum sidelobe decay windows – theory and properties: a review and new results. *Metrology and Measurement Systems*, 751. https://doi.org/10.24425/mms.2024.150294

[20] Borkowski, J., Mroczka, J., Matusiak, A., & Kania, D. (2020). Frequency estimation in interpolated discrete fourier transform with generalized maximum sidelobe decay windows for the control of power. *IEEE Transactions on Industrial Informatics*, *17*(3), 1614–1624. https://doi.org/10.1109/tii.2020.2998096

[21] Loock, H., & Wentzell, P. D. (2012). Detection limits of chemical sensors: Applications and misapplications. *Sensors and Actuators B Chemical*, *173*, 157–163. https://doi.org/10.1016/j.snb.2012.06.071

Sławomir Cięszczyk is an associate professor at the Department of Electronics and Information Technology at the Lublin University of Technology. He received the Ph.D. degree in 2008 and the D.Sc. Degree in habilitation in 2018. His research interests include optical sensors, open-path spectroscopy, signal processing, data analysis, numerical methods, simulation and modeling.

Krzysztof Skorupski received the M.Sc. degree in 2004 from Lublin University of Technology (LUT), Poland and Ph.D. from AGH University of Krakow in 2017. He is currently an assistant professor at LUT. His research interests are in the field of inscription and applications of fibre Bragg gratings.

Metrol. Meas. Syst., Vol. 32 (2025), No. 3
DOI: 10.24425/mms.2025.154680

Patryk Panas received the M.Sc. degree in Mechatronics in 2017 from the Faculty of Electrical Engineering and Computer Science at the Lublin University of Technology (LUT). At this moment he is employed as an assistant professor at the same university. He is involved in the implementation of optical fibre sensors based on fibre Bragg gratings.

Martyna Wawrzyk is PhD student, M. Eng of Biomedical Engineering at Lublin University of Technology in the Faculty of Electrical Engineering and Computer Science. The author several articles about biomedical signal processing, data analysis, data classification and spectrum analysis. Her current research interests include algorithms applied in pre-processing of data, for example filtering data or baseline correction. Additionally, her other scientific interests involve analysis spectrum of optical data and open path FT-IR spectroscopy.